Syndromes with aortic involvement: pictorial review

Evan J. Zucker

Department of Radiology, Stanford University School of Medicine, Stanford, CA, USA

Correspondence to: Evan J. Zucker, MD. Department of Radiology, Stanford University School of Medicine, 725 Welch Road, Stanford, CA 94305, USA. Email: zucker@post.harvard.edu.

Abstract: A variety of syndromes are associated with thoracoabdominal aortic pathologies. While these diseases are collectively rare, the presence of advanced or unusual aortic disease at a young age should raise suspicion of an underlying syndrome. Similarly, patients with a known syndrome require close monitoring in anticipation of future aortic disease. In this article, the syndromes most commonly encountered in clinical practice are reviewed, including Marfan syndrome (MFS) and other connective tissue disorders, Turner syndrome (TS), autosomal dominant polycystic kidney disease (ADPKD), neurofibromatosis (NF), Williams syndrome (WS), Alagille syndrome (AGS), and DiGeorge syndrome (DGS). The distinct clinical, imaging, and management features of each disorder are discussed. Attention is focused on the unique patterns of aortic disease in each syndrome, emphasizing the role of recent imaging modalities and treatment strategies. Ancillary and distinguishing aspects of the syndromes that aid in diagnosis are also highlighted.

Keywords: Aorta; syndrome; Marfan; Turner; Williams; Alagille

Introduction

Most aortic diseases encountered in routine clinical practice are acquired, occurring most commonly in the older adult population. However, acquired pathology such as aneurysm formation or dissection at a young age, unusual patterns of aortic disease, or a congenital aortic anomaly should raise suspicion for an underlying syndrome. While such syndromes are rare, it is well-established that many aortic diseases likely have a genetic predisposition. For example, individuals who have a first-degree relative with an aortic aneurysm are at 10–12 times the risk of a developing aneurysms themselves (1-4).

In recent years, a variety of genetic syndromes predisposing to aortic pathology have been recognized. While comprising only a small subset of hereditary aortic diseases, the known syndromes are encountered with sufficient frequency to merit special study and attention. Of these, Marfan syndrome (MFS), and other connective tissue disorders such as Ehlers-Danlos syndrome (EDS) and Loeys-Dietz syndrome (LDS), are likely seen most often. Other disorders presenting not uncommonly include Turner

syndrome (TS), autosomal dominant polycystic kidney disease (ADPKD), and neurofibromatosis (NF), as well as Williams syndrome (WS), Alagille syndrome (AGS), and DiGeorge syndrome (DGS) (1).

Herein, the most commonly encountered syndromes with aortic involvement are reviewed. Emphasis is placed on their unique patterns and presentations of aortic pathology and associated unique imaging appearances and management strategies. Genetic and pathophysiological underpinnings of each disorder and distinctive associated features are also highlighted.

Connective tissue disease

Collagen and elastin are among the most crucial structural proteins that ensure vascular wall integrity. Thus, it is not surprising that connective disorders associated with mutations in genes encoding these proteins are linked to aortic disease, including degeneration, dissection, and aneurysm formation. The most commonly encountered genetic connective tissue disorders include MFS, vascular EDS (type IV), LDS, and familial aortic aneurysms and
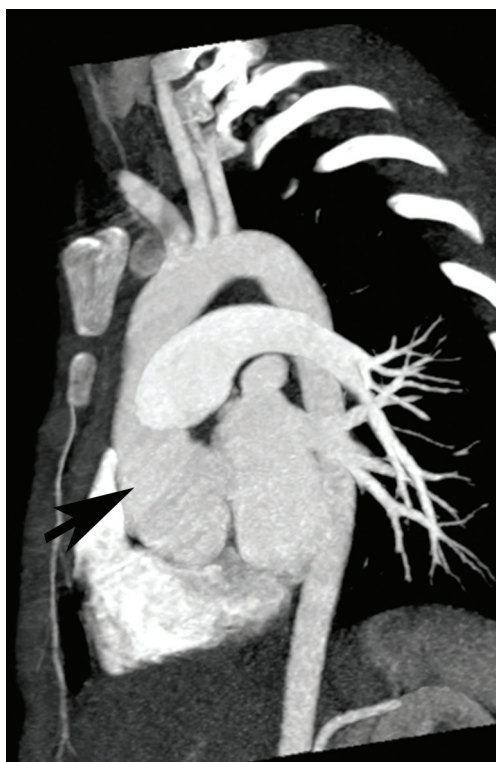
Figure 1 Marfan syndrome. A 7-year-old male with Marfan syndrome referred for thoracic aortic evaluation. Maximum intensity projection (MIP) reformatted image from a chest computed tomography angiography (CTA) examination shows an aneurysmal aortic root (arrow) with effacement of the sinotubular junction, producing the so-called "tulip bulb" appearance.

dissections, herein discussed (5).

MFS

MFS is caused by autosomal dominant mutations in the fibrillin-1 (*FBN1*) gene on chromosome 15q21.1. *FBN1* codes for an extracellular matrix protein that helps facilitate the attachment of smooth muscle to collagen and elastin matrices and in turn the integrity of the aortic wall (5,6). When *FBN1* is deficient, transforming growth factor-β (TGFB) activity increases, resulting in inflammation and fibrosis of the aorta and in turn dilation and aneurysm development (6). Another subtype of MFS (MFS2) is caused by direction mutations in the TGFB receptor 2 (TGFBR2) (1,6).

Not uncommon, MFS has a prevalence of 1–3 in 10,000 (1,5). It is a multiorgan system disease including cardiovascular, ocular, and musculoskeletal involvement, sometimes also with neurologic, pulmonary, or dermatologic effects (1,7). MFS diagnosed based on a set of diverse possible clinical findings known as the revised Ghent criteria (6). Approximately 70–93% of patients who meet these criteria possess an *FBN1* mutation, although more than 600 *FBN1* mutations have been identified (1).

The cardiovascular manifestations of MFS are among the most critical in affecting the prognosis, with almost 80% of the disease's morbidity attributed to aortic aneurysm formation and dissection (1,5,8). The aortic annulus, root, and ascending aorta are most commonly affected with progressive dilation, although more of the thoracic aorta may be involved with time (6). In fact, the sinuses of Valsalva are known to dilate even during fetal life (5). As the aorta grows in size, the risk for dissection and rupture increases. In adults, prophylactic surgery is recommended for aortic root diameters ≥5 cm, although in experienced centers, the threshold may be lowered to diameters ≥4.5 cm. Regardless, elective surgery is recommended for diameters <5 cm with growth ≥0.5 cm/year (5,9). In children, guidelines are less well established but severe aortic insufficiency, aortic growth >1 cm/year, or aortic size Z-score of >2–3 are concerning features (5). Other cardiovascular manifestations of MFS may include mitral valve prolapse that can lead to valvular insufficiency or endocarditis, myocardial dysfunction that may precipitate heart failure and sudden cardiac death, and rarely pulmonary artery (PA) enlargement that can lead to dissection or rupture (7).

Annual imaging of the aortic root is recommended in MFS (9,10). This may be performed with echocardiography, computed tomography angiography (CTA), or magnetic resonance angiography (MRA) (*Figures 1* and *2*). Although widely available and essentially risk-free, echocardiography is operator-dependent and cannot assess the entirety of the aorta. The decision to use CT *vs.* magnetic resonance imaging (MRI) for aortic measurements is mostly institution-dependent. Advantages of CT include rapid acquisition and excellent spatial resolution such as for pre-surgical planning, while downsides include exposure to ionizing radiation and the need for intravenous contrast. MRA provides essentially equivalent information, although imaging tends to be longer and more prone to artifact in patients with prior surgery. However, it poses no radiation risk and can be performed without contrast (9,11,12). Both modalities allow multiplanar and three-dimensional (3D) reconstruction. If indicated, MR phase contrast techniques can also assess the severity of any associated aortic regurgitation. Newer four-dimensional (4D) flow MR techniques now also allow assessment of aortic flow

Figure 2 Marfan and Turner syndromes. A 41-year-old female with both Turner and Marfan syndromes post repair for aortic dissection. Sagittal post-gadolinium magnetic resonance angiography (MRA) image shows post-surgical changes of the aorta (arrow) with residual descending aortic dissection flap (asterisk).

Figure 3 Ehlers-Danlos syndrome. A 60-year-old female with a history of Ehlers-Danlos syndrome. Sagittal post-gadolinium MRA image shows mild ectasia of the aortic root (arrow).

patterns, which may help better predict the risk of future dissection (13,14).

EDS

EDS refers to a heterogeneous spectrum of genetic disorders characterized by defective collagen synthesis, leading to joint hypermobility, skin hyperextensibility, and tissue fragility (5,6). There are over 10 recognized subtypes, although more recently the disease has been grouped into 7 major categories: classical, hypermobility, vascular, kyphoscoliosis, arthrochalasia, dermatosparaxis, and other (1,5). Of these, vascular EDS (type IV) is, as the name implies, most strongly associated with cardiovascular complications. Vascular EDS, with a prevalence of 1 in 100,000–250,000, is caused by autosomal dominant mutations in the type III procollagen (*COL3A1*) gene, leading to deficits in the most abundant type of collagen usually found in the aorta extracellular matrix and resultant vascular fragility and risk of rupture (5,6). Other clinical features include characteristic facies (tight and translucent skin, thin lips, pinched nose, prominent ears, hollow

cheeks) and easy bruising (1,6). Patients are also at risk for intestinal and uterine rupture in pregnancy (1). Vascular complications may also be seen with the classical and hypermobile forms of EDS but to a much lesser extent (1,5).

In contrast to MFS, vascular EDS typically involves thoracoabdominal medium-sized arteries, often the descending or abdominal aorta (1,5). Moreover, patients are at risk for rupture regardless of vessel diameter. In fact, development of true aneurysms is rare in the disease. Because of the high rate of vascular rupture, the mean life expectancy is 48 years (in contrast to 60 years for MFS) (5). In one series of >200 vascular EDS patients, 60% died by age 40 years; in 60% of these cases, the cause of death was aortic rupture (5,15).

Because of the marked vessel friability in vascular EDS, noninvasive imaging modalities, including ultrasound, CT, and MRI are much preferred to catheter-based angiography that could precipitate rupture (*Figure 3*) (1,16). While imaging accurately depicts complications of EDS, no modality can currently predict the risk of rupture in asymptomatic patients. Management is controversial, although patients generally are advised to receive genetic
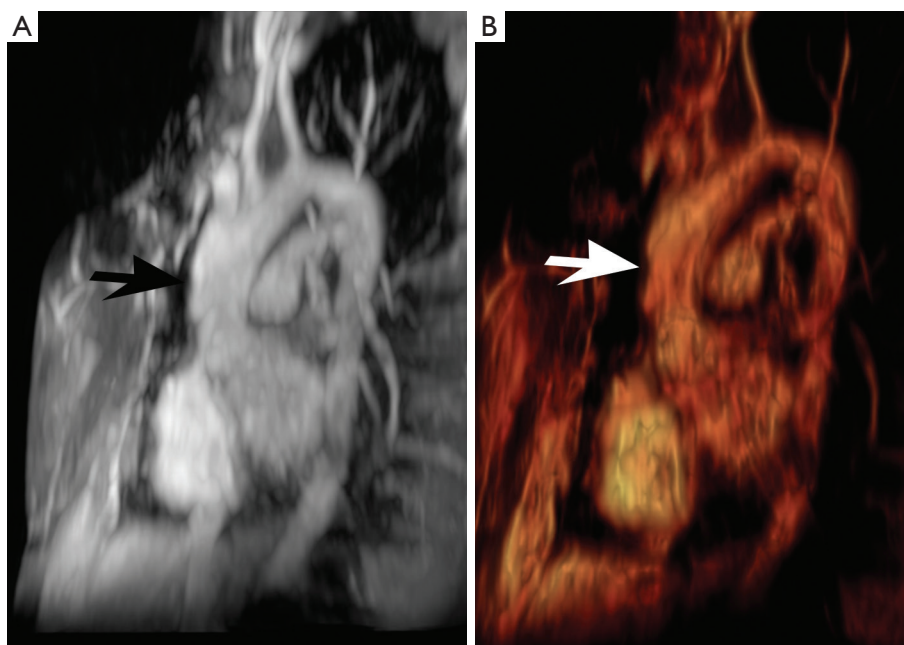
Figure 4 Loeys-Dietz syndrome. A 16-year-old female with Loeys-Dietz syndrome post aortic repair. (A) MIP and (B) 3D reformatted post-contrast MRA images show a normal caliber aortic root and ascending aorta (arrows) post repair.

and cardiovascular evaluation and vigilant monitoring (16). Aortic size ≥4.4 cm is a suggested size cutoff for surgery (6). Minimally invasive procedures were once felt completely contraindicated due to the risk of vascular rupture or other complications related to arterial puncture and catheter manipulation; however, some report success with such techniques (1,6).

LDS

LDS is an aggressive disorder caused by heterozygous mutations in TGFB receptors 1 or 2 (TGFBR1/TGFBR2). This leads to excess collagen production with loss of elastin and elastic fiber disorganization (1,5). Although precise diagnostic criteria have not been established, the disease is grouped into 2 major subtypes. Type 1 has Marfan-like features including marked craniofacial and skeletal abnormalities, while type 2 resembles vascular EDS including the presence of a bifid uvula and potential complications in pregnancy. Common to both are vascular abnormalities, including aortic root and other aneurysms, arterial tortuosity, and dissections (1,5,6).

There are several unique features of vascular involvement in LDS. Unlike the expected course of MFS but similar to that of vascular EDS, aortic dissection and rupture may

occur at small diameters (5,6). In fact, aortic aneurysms are only seen in an estimated 9% of patients. However, the aorta can rapidly increase size, such as at a rate of 1.8 mm/year. The infrarenal abdominal aorta is typically twice normal size but usually non-aneurysmal (5).

LDS rivals vascular EDS in its aggressive nature. However, LDS has a much more favorable perioperative mortality rates compared to vascular EDS (1.7% *vs.* 45%, respectively) (1). Thus, close surveillance imaging with at least annual echocardiography is felt prudent in LDS (17). Moreover, early and frequent surgery is often pursued, including a suggestion for prophylactic repair of aortic diameters ≥4–4.4 cm (1,6,18). Serial imaging also assists in monitoring post multiple interventions (*Figure 4*) (17). Nevertheless, the prognosis is poor, with a median survival age of 37 years (1).

Familial thoracic aortic aneurysms and dissections (FTAAD)

This spectrum of disorders (FTAAD) describes familial associations of typically ascending aortic aneurysms and dissection in the absence of an identifiable syndromes or other characteristic phenotypic features (1,6). As many as 1 in 5 thoracic aortic aneurysms are believed to have a
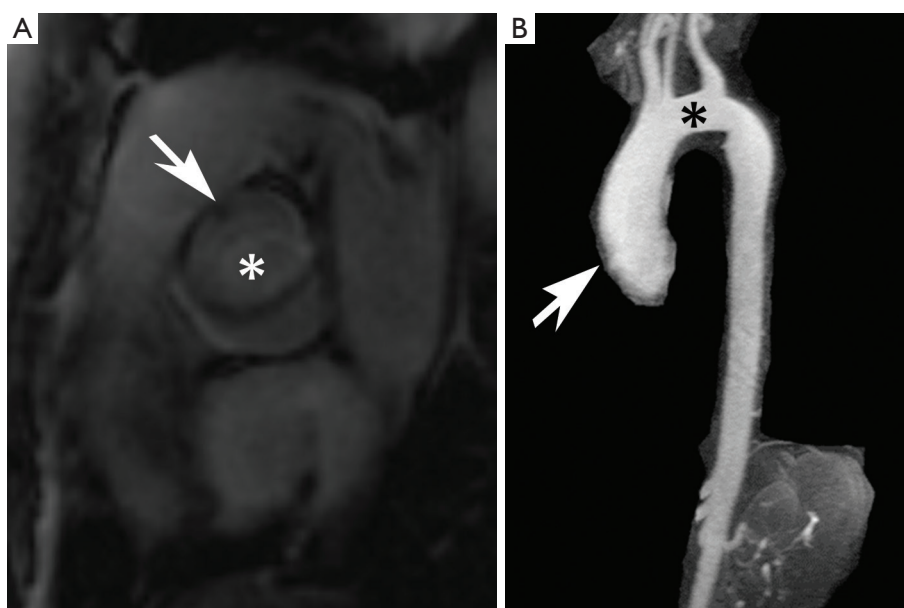
Figure 5 Turner syndrome. A 36-year-old female with Turner syndrome undergoing routine imaging evaluation. Balanced steady-state free precession (bSSFP) ("bright blood") image (A) of the aortic valve (asterisk) shows bicuspid morphology. There is a raphe (arrow) fusing the left and right cusps, indicating a Sievers type 1/L-R bicuspid valve. MIP reformatted image (B) from a contrast-enhanced MRA shows borderline dilation of the aortic root (arrow) and elongation of the aortic arch (asterisk).

heritable basis, although only a small number of candidate genes have been identified. These include genes that affect TGFB pathways such as *SMAD3* and others that facilitate smooth muscle contraction (such as *ACTA2*, *MYH11*, *MYLK*, and *PRKG1*) (6). Overall, aneurysms tend to arise approximately 10 years earlier in patients with FTAAD compared to those without an identifiable family history (1). Because of the heterogeneity of this condition, there is a lack of specific management recommendations (6). While screening asymptomatic individuals with a suspected familial aortopathy may reveal unsuspected aneurysms, a normal aortic diameter does not preclude the development of subsequent disease (19). Although echocardiography is the typical first-line, when nondiagnostic, other modalities such as CT or MRI can be pursued.

TS

TS is an aneuploidy disorder characterized by complete or partial absence of one X chromosome, typically resulting in a 45,X karyotype (1,20). Affecting 1 in 2,000–2,500 females, TS is associated with a variety of cardiovascular abnormalities, including bicuspid aortic valve, aortic coarctation, aortic root dilation/aneurysm formation,

and aortic arch elongation as well as persistent left superior vena cava and partial anomalous pulmonary venous return (PAPVR) (*Figures 2* and *5*) (1,20,21). Additional arteries may dilate including the carotid and brachial arteries (1). Overall, congenital or acquired cardiovascular pathology arises in as much as half of TS patients, associated with dissections occurring at a mean age of 30 years that portend 3 times the age-specific mortality rate. The etiology of these abnormalities may be related to abnormal TGFB signaling (21). Other typical clinical features in TS include short stature and lack of normal gonadal formation (20).

Because TS conveys an increased risk of aortic dilation as well as dissection, regular surveillance imaging is advised (20,22). While transthoracic echocardiography is the first-line diagnostic modality, it may be limited at older ages and may underdiagnose PAPVR and progression of aortic dilation (20,23-25). MRI has therefore been suggested as useful adjunct and provides reliable assessment of aortic dimensions and morphology (20,22,23,25). CT could also be used for these purposes. As in other disorders, 4D flow MRI techniques have been used to noninvasively evaluate aortic flow trajectories in patients with TS; early research suggests altered patterns of wall shear stress that may contribute to disease (21).
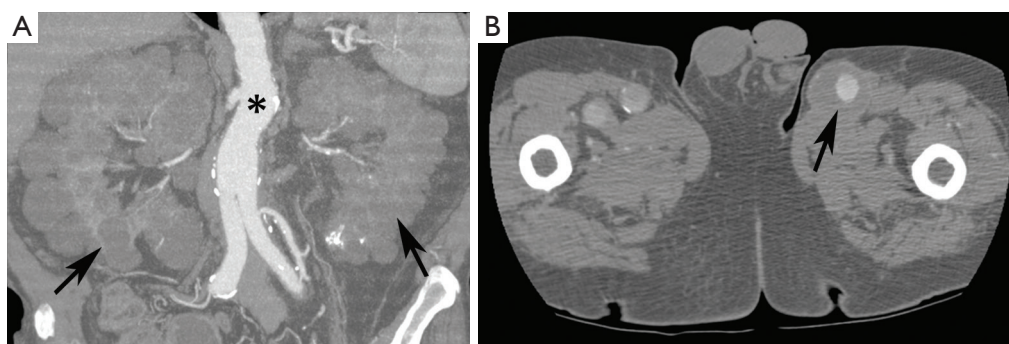
Figure 6 Autosomal dominant polycystic kidney disease (ADPKD). A 72-year-old male with ADPKD post abdominal aortic repair presenting with a left groin lump. MIP reformatted image (A) from a CTA shows a patent aortoiliac bypass graft (asterisk). Note the enlarged kidneys (arrows) with innumerable bilateral cysts. Axial image (B) from the same CTA shows a partially thrombosed left common femoral artery aneurysm (arrow), the etiology of the "groin lump".

ADPKD

ADPKD is caused by mutations in the *PKD1* (85%) or *PKD2* (15%) genes, which code for polycystin proteins that function in calcium channel development (1). It is among the most common heritable disorders, with a prevalence in 1 in 400–1,000 (1,26). While the disease is most known for the development of enlarged kidneys with multiple bilateral cysts, a number of non-cystic abnormalities occur (1). Among these are cardiovascular manifestations, including intracranial aneurysms and dolichoectasia, aortic and cervicocephalic artery aneurysms and dissections, coronary artery aneurysms, atrial septal aneurysms, and mitral valve prolapse (*Figure 6*) (1,26,27). Bicuspid aortic valve, aortic coarctation, and even interrupted aortic arch have been described in association with ADPKD (28). Polycystins are present on vascular smooth muscle and endothelial cells on all major vessels, including the intracranial arteries and aorta, and are thought to help ensure vessel wall integrity; these factors may thus explain the association between ADPKD and vascular disease (1).

Screening for intracranial aneurysms in ADPKD is common practice, usually with non-contrast MRA (or if nondiagnostic or contraindicated, contrast-enhanced MRA or CTA) at diagnosis and then every 2–10 years. Data on screening for other vascular pathology is limited, and thus firm recommendations cannot be made. However, screening may be reasonable in an ADPKD patient with a family history of a specific vascular abnormality such as aortic dilation (26). Moreover, vascular complications such as aortic dissection should be suspected in symptomatic patients with ADPKD despite their young age (27). As in other disorders,

such findings are well demonstrated by CT and MRI.

NF

NF is an autosomal dominant genetic neurocutaneous disorder (phakomatosis) with 2 types (NF1 and NF2). NF1, or von Recklinghausen disease, occurs with greater frequency and is characterized by mutations in the *NF1* gene found on chromosome 17q11.2. The overall prevalence is 1 in 3,000–4,000 (1,29). The diagnosis is based on a set of criteria established by the National Institutes of Health (NIH) consisting of characteristic clinical findings such as café-au-lait spots, iris hamartomas (Lisch nodules), optic glioma, axillary freckling, dermal neurofibromas, or a distinctive skeletal abnormality (e.g., sphenoid wind dysplasia) and a first-degree relative with NF1. Two or more of these features (in specified numbers) establish the diagnosis (29,30).

NF1 is associated with a variety of vascular abnormalities. This so-called "NF1 vasculopathy" is estimated to arise in 0.4–6.4% of patients diagnosed with NF1. The *NF1* gene codes for a tumor-suppressor protein known as neurofibromin that is expressed on tissues throughout multiple organ systems, including blood vessels. Mutations in neurofibromin lead to abnormal endothelial and smooth muscle development, in turn altering normal vessel structural maintenance processes and causing intimal thickening and disarray (29,31). Renal artery stenosis is the most common vascular abnormality in NF1, followed by abdominal coarctation/midaortic syndrome (*Figure 7*) (2,29-31). However, vascular lesions including aneurysm formation or occlusion of any artery throughout the cerebro- and cardiovascular systems may occur (*Figure 8*) (30).
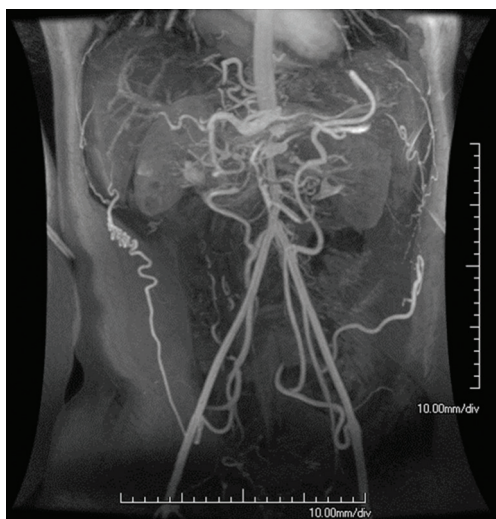
Figure 7 Midaortic syndrome. A 35-year-old male with history of multiple stenoses. MIP reformatted image from a gadolinium-enhanced MRA shows long segment severe stenosis of the abdominal aorta with collateral formation. These findings are consistent with midaortic syndrome.
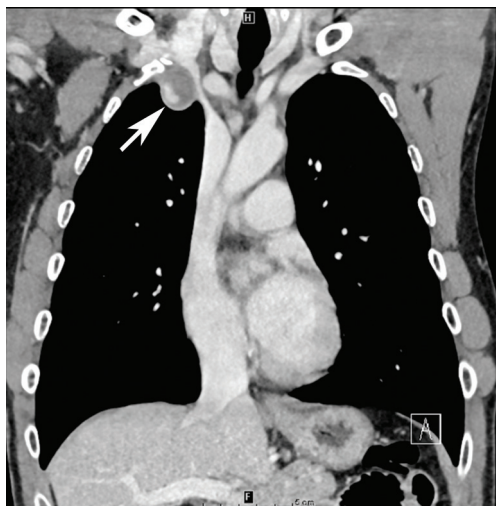
Figure 8 Neurofibromatosis type 1. A 33-year-old male with NF1. Coronal CTA image shows a partially thrombosed aneurysm (arrow) of the right internal mammary artery.

Although patients with NF1 are prone to vascular abnormalities, the frequency of such findings remains low; thus, routine screening for vasculopathy in NF1 patients is not currently recommended. However, an imaging evaluation of the head, chest, and abdomen, should be prompted if an NF1 patient has hypertension (29). A

variety of modalities, including initially echocardiography followed by CT or MRI can be used for these purposes (30,31). Surgical or endovascular techniques can be used for treatment, depending on the lesion (29-31).

WS

WS, also known as Williams-Beuren syndrome (named for the authors who first reported it), is a multiorgan system disorder caused by deletions, usually *de novo*, on chromosome 7q11.23 (32,33). It arises in approximately 1 in 10,000 live births (32,34,35). Classic clinical features include "elfin facies," hypercalcemia, and overall mental retardation with relatively preserved verbal skills including a cheerful, outgoing personality (32).

Cardiovascular abnormalities feature prominently in WS, occurring in 80% of patients (32,36). These are attributed to deficient elastin protein, whose gene is among the deleted segment in WS; elastin normally helps to counteract arterial stiffness and regulate vascular smooth muscle (32). The most frequent cardiovascular anomalies in WS include supravalvular aortic stenosis, pulmonary arterial stenosis, and coronary artery ostial stenosis (*Figure 9*) (32,36,37). Other findings may include mitral valve prolapse, aortic coarctation, subaortic stenosis, a ventricular septal defect or patent foramen ovale, and hypertrophic cardiomyopathy (32,36). Because WS leads to a generalized vasculopathy of large and medium-sized arteries, stenoses or occlusions may be seen in vessels spanning from the head and neck through the abdomen (36).

Due to the high prevalence of cardiovascular disease in WS, it is recommended that all Williams patients be referred to a pediatric cardiologist for a complete evaluation, including four-extremity blood-pressures, electrocardiography, and echocardiography. If an arterial stenosis is suspected based on physical findings (hypertension, bruit, etc.) or echocardiography, further imaging may be needed, such as CT, MRI, or invasive angiography (32). CT may be preferred because it can provide excellent noninvasive evaluation of the coronary arteries with lower doses compared to angiography (36). While many stenoses in WS can be expectantly monitored with serial surveillance imaging, ultimately 20% of patients require a transcatheter or surgical intervention by age 15 years (32,38-40).

AGS

AGS is a genetic, autosomal dominant, multisystem
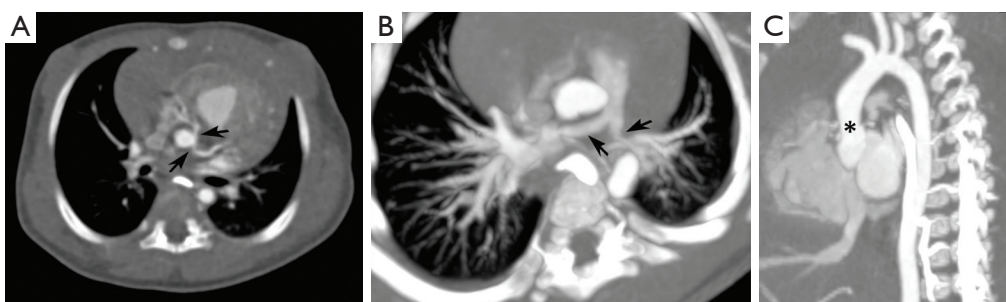
Figure 9 Williams syndrome. A 12-week-old male with Williams syndrome undergoing preoperative imaging evaluation. Axial image (A) from a non-gated chest CTA shows ostial narrowing (arrows) of the coronary arteries. MIP reformatted image (B) shows diffusely small bilateral pulmonary arteries (arrows). MIP reformatted image in candy-cane orientation (C) shows mild narrowing of the supravalvular thoracic aorta (asterisk).
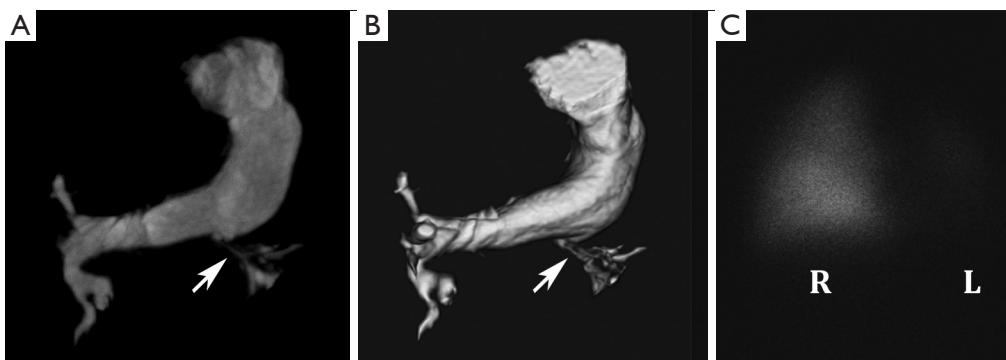
Figure 10 Alagille syndrome. A 2-year-old male with Alagille syndrome referred for preoperative imaging. MIP (A) and 3D reformatted (B) CTA images show an extremely small and stenotic left pulmonary artery (arrows). Nuclear medicine pulmonary perfusion scan (C) after administration of technetium 99mTc macro aggregated albumin (99mTc-MAA) shows nearly absent perfusion to the left lung (L) compared to the right lung (R).

disorder, caused by mutations in *JAG1* or *NOTCH2*, both involved in Notch signaling pathways (41). It arises in 1 in 70,000 newborns (42). Biliary cirrhosis related to deficient intrahepatic bile ducts is a central feature of the disease, leading to liver transplantation in up to half of patients (41). Other clinical features include abnormal facies and skeletal anomalies such as butterfly vertebrae and posterior embryotoxon of the eye (a corneal posterior ring) (40,41).

Notch signaling pathways are involved in angiogenesis, and thus it is not surprising that vascular findings also feature prominently in AGS (43). Peripheral PA stenoses are the most common vascular abnormality, occurring in more than 3 in 4 AGS patients (41,42). The characteristic PA features include: small right and left central PAs relative to the main PA, a left PA that is generally significantly smaller compared to the right PA (*Figure 10*), and high-

grade stenoses involving numerous lobar and segmental PA branches, more so in the upper lungs, with the right lung more affected than the left (42). Beyond PA anomalies, a variety of other vascular abnormalities may be seen, including aortic coarctation and aneurysms, intracranial and internal carotid artery aneurysms, and renal, celiac, hepatic, superior mesenteric, or subclavian artery stenosis (44).

Although firm guidelines are not available, it is considered prudent to rigorously investigate potential vascular anomalies in AGS patients with pertinent symptoms (e.g., hypertension, neurologic deficits) (44). The high frequency of PA involvement inevitably requires imaging evaluation; CT provides an excellent noninvasive anatomical assessment for these purposes may be supplemented by lung perfusion scintigraphy to determine the relative blood flow to each lung and cardiac catheterization to measure intracardiac
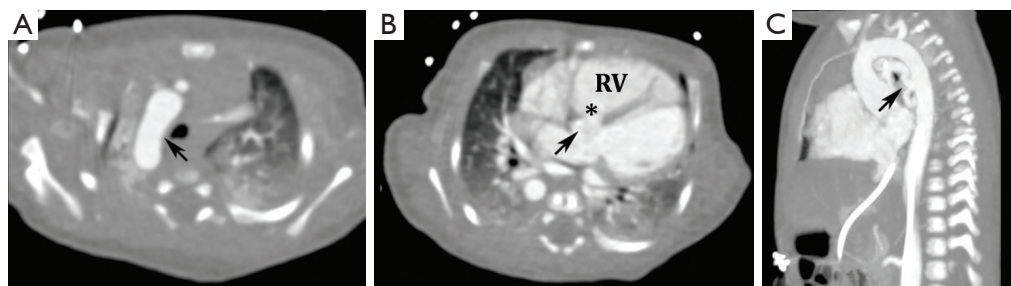
Figure 11 DiGeorge syndrome. A 2-day-old male with DiGeorge syndrome and complex congenital heart disease undergoing preoperative evaluation. Axial CTA images show a right aortic arch (A, arrow) and tetralogy of Fallot morphology (B), including a dilated right ventricle (RV), malalignment ventricular septal defect (asterisk), and overriding aorta (arrow). MIP reformatted image (C) shows large-caliber major aortopulmonary collaterals (arrow) that arise from the descending aorta and supply the pulmonary arterial circulation in this patient who also had pulmonary atresia.

pressures (43). CT or MRI can be used to assess other potential areas of involvement, depending on symptoms and abnormal sonographic findings (45). Catheter-based and surgical options have shown good results in treating PA abnormalities (46). Treatment for other vascular abnormalities is tailored to the sites of involvement.

DGS

Arising in 1 in 4,000–10,000 births, DiGeorge or velocardiofacial syndrome is usually caused by a chromosome 22q11.2 microdeletion (47-50). Its typical clinical features can be recalled with the mnemonic "CATCH 22," an acronym for: cardiac disease, abnormal facies, thymic hypoplasia, cleft palate, and hypocalcemia, associated with a chromosome 22 deletion. While the syndrome can be inherited, it more commonly arises *de novo* (48).

Cardiovascular abnormalities are prominent features of DGS; in fact, congenital heart disease and aortic arch anomalies arise in more than 4 in 5 patients (49). The spectrum of potential anomalies is diverse but along the spectrum of conotruncal and branchial arch malformations. Abnormalities may include: tetralogy of Fallot, interrupted aortic arch, infundibular malalignment ventricular septal defects, aortic arch aberrations including vascular rings, aortic root dilation, and truncus arteriosus (*Figure 11*) (48,51). It is postulated that defects in the ubiquitin-fusion-degradation-1-like (*UFD1L*) gene that is normally present in the segment deleted in DiGeorge lead to abnormal conotruncal and arch embryogenesis, allowing for this unique set of malformations (48,49).

While echocardiography is generally well-suited for assessing intracardiac anatomy, CT and MRI are often superior for assessment of malformations involving large vessels such as the aorta. Moreover, these modalities can provide a better understanding of 3D relationships that may be required for presurgical planning (52). Management varies according to the anomalies involved. Of note, because conotruncal anomalies are so strongly associated with DiGeorge, it is recommended that children with a conotruncal abnormality be specifically tested for this syndrome (48).

Conclusions

A broad spectrum of genetic syndromes involve the aorta and other large arteries. While cardiovascular phenotypes overlap, unique features of disorders encountered with frequency in a subspecialty practice should be remembered. These include: aortic root and ascending aortic dilation and dissection in connective tissue disorders such as MFS; coarctation, bicuspid aortic valve, and aortic arch elongation in TS; intracranial and cervicocephalic aneurysms in ADPKD; renal artery stenosis and mid-aortic syndrome in NF1; supravalvular aortic, coronary, and pulmonary stenoses in Williams syndrome; peripheral PA stenosis sometimes accompanied by involvement of other arteries in AGS; and conotruncal and arch anomalies in DGS. The pathogenesis of these diverse abnormalities is generally attributed to specific gene deficiencies, leading to malformations in vessel development. While echocardiography remains the first-line imaging modality, CT and MRI are often optimally suited for assessing large artery anomalies and have been adopted with increasing frequency. The syndromes described in this review represent only a small subset of the many entities, named and unnamed, causing distinctive aortic pathologies. With continued advances in genetic knowledge and imaging

modalities, the scope of knowledge should only continue to increase.

Acknowledgements

Footnote

Conflicts of Interest: The author has no conflicts of interest to declare.

References

1. Cury M, Zeidan F, Lobato AC. Aortic disease in the young: genetic aneurysm syndromes, connective tissue disorders, and familial aortic aneurysms and dissections. Int J Vasc Med 2013;2013:267215.
2. Majumder PP, St Jean PL, Ferrell RE, et al. On the inheritance of abdominal aortic aneurysm. Am J Hum Genet 1991;48:164-70.
3. Sandford RM, Bown MJ, London NJ, et al. The genetic basis of abdominal aortic aneurysms: a review. Eur J Vasc Endovasc Surg 2007;33:381-90.
4. Webster MW, St Jean PL, Steed DL, et al. Abdominal aortic aneurysm: results of a family study. J Vasc Surg 1991;13:366-72.
5. Böckler D, Meisenbacher K, Peters AS, et al. Endovascular treatment of genetically linked aortic diseases. Gefasschirurgie 2017;22:1-7.
6. Sun JC. Genetic disorders of the thoracic aorta and indications for surgery. Cardiol Clin 2017;35:317-20.
7. von Kodolitsch Y, De Backer J, Schüler H, et al. Perspectives on the revised Ghent criteria for the diagnosis of Marfan syndrome. Appl Clin Genet 2015;8:137-55.
8. Porciani MC, Attanasio M, Lepri V, et al. Prevalence of cardiovascular manifestations in Marfan syndrome. Ital Heart J Suppl 2004;5:647-52.
9. von Kodolitsch Y, Rybczynski M, Detter C, et al. Diagnosis and management of Marfan syndrome. Future Cardiol 2008;4:85-96.
10. Veldhoen S, Behzadi C, Derlin T, et al. Exact monitoring of aortic diameters in Marfan patients without gadolinium contrast: intraindividual comparison of 2D SSFP imaging with 3D CE-MRA and echocardiography. Eur Radiol 2015;25:872-82.
11. Krishnam MS, Tomasian A, Malik S, et al. Image quality and diagnostic accuracy of unenhanced SSFP

12. Lindsay AC, Sriharan M, Lazoura O, et al. Multidetector computed tomography of congenital aortic abnormalities. Int J Cardiol 2014;172:537-47.
13. Geiger J, Hirtler D, Gottfried K, et al. Longitudinal evaluation of aortic hemodynamics in Marfan syndrome: new insights from a 4D flow cardiovascular magnetic resonance multi-year follow-up study. J Cardiovasc Magn Reson 2017;19:33.
14. van der Palen RL, Barker AJ, Bollache E, et al. Altered aortic 3D hemodynamics and geometry in pediatric Marfan syndrome patients. J Cardiovasc Magn Reson 2017;19:30.
15. Pepin M, Schwarze U, Superti-Furga A, et al. Clinical and genetic features of Ehlers-Danlos syndrome type IV, the vascular type. N Engl J Med 2000;342:673-80.
16. Soo-Hoo S, Porten BR, Engstrom BI, et al. Ehlers-Danlos syndrome type IV: a case report. Vasc Endovascular Surg 2016;50:156-9.
17. Patel ND, Alejo D, Crawford T, et al. Aortic root replacement for children with Loeys-Dietz syndrome. Ann Thorac Surg 2017;103:1513-8.
18. Williams JA, Loeys BL, Nwakanma LU, et al. Early surgical experience with Loeys-Dietz: a new syndrome of aggressive thoracic aortic aneurysm disease. Ann Thorac Surg 2007;83:S757-63.
19. Hannuksela M, Stattin EL, Johansson B, et al. Screening for familial thoracic aortic aneurysms with aortic imaging does not detect all potential carriers of the disease. Aorta (Stamford) 2015;3:1-8.
20. Kim HK, Gottliebson W, Hor K, et al. Cardiovascular anomalies in Turner syndrome: spectrum, prevalence, and cardiac MRI findings in a pediatric and young adult population. AJR Am J Roentgenol 2011;196:454-60.
21. Arnold R, Neu M, Hirtler D, et al. Magnetic resonance imaging 4-D flow-based analysis of aortic hemodynamics in Turner syndrome. Pediatr Radiol 2017;47:382-90.
22. Yiğit H, Önder A, Özgür S, et al. Cardiac MRI and 3D contrast-enhanced MR angiography in pediatric and young adult patients with Turner syndrome. Turk J Med Sci 2017;47:127-33.
23. Dawson-Falk KL, Wright AM, Bakker B, et al. Cardiovascular evaluation in Turner syndrome: utility of MR imaging. Australas Radiol 1992;36:204-9.
24. Masui T, Seelos KC, Kersting-Sommerhoff BA, et al. Abnormalities of the pulmonary veins: evaluation with MR imaging and comparison with cardiac angiography and

MR angiography compared with conventional contrast-enhanced MR angiography for the assessment of thoracic aortic diseases. Eur Radiol 2010;20:1311-20.

echocardiography. Radiology 1991;181:645-9.

25. Hjerrild BE, Mortensen KH, Sørensen KE, et al. Thoracic aortopathy in Turner syndrome and the influence of bicuspid aortic valves and blood pressure: a CMR study. J Cardiovasc Magn Reson 2010;12:12.

26. Perrone RD, Malek AM, Watnick T. Vascular complications in autosomal dominant polycystic kidney disease. Nat Rev Nephrol 2015;11:589-98.

27. Silverio A, Prota C, Di Maio M, et al. Aortic dissection in patients with autosomal dominant polycystic kidney disease: a series of two cases and a review of the literature. Nephrology (Carlton) 2015;20:229-35.

28. Seker Koçkara A, Kayataş M, Huzmeli C, et al. Interrupted aortic arch in an adult with polycystic kidney disease. Case Rep Med 2013;2013:404710.

29. Mavani G, Kesar V, Devita MV, et al. Neurofibromatosis type 1-associated hypertension secondary to coarctation of the thoracic aorta. Clin Kidney J 2014;7:394-5.

30. Kimura M, Kakizaki S, Kawano K, et al. Neurofibromatosis type 1 complicated by atypical coarctation of the thoracic aorta. Case Rep Pediatr 2013;2013:458543.

31. Veean S, Thakkar N, Gupta S, et al. A case of coarctation of the abdominal aorta and renal artery stenosis due to neurofibromatosis type 1. Postgrad Med J 2017;93:235-6.

32. Collins RT 2nd. Cardiovascular disease in Williams syndrome. Circulation 2013;127:2125-34.

33. Kaplan P, Wang PP, Francke U. Williams (Williams Beuren) syndrome: a distinct neurobehavioral disorder. J Child Neurol 2001;16:177-90.

34. Strømme P, Bjørnstad PG, Ramstad K. Prevalence estimation of Williams syndrome. J Child Neurol 2002;17:269-71.

35. Federici D, Ranghetti A, Merlo M, et al. Coronary artery involvement of Williams syndrome in infants and surgical revascularization strategy. Ann Thorac Surg 2016;101:359-61.

36. Das KM, Momenah TS, Larsson SG, et al. Williams-Beuren syndrome: computed tomography imaging review. Pediatr Cardiol 2014;35:1309-20.

37. Pieles GE, Ofoe V, Morgan GJ. Severe left main coronary artery stenosis with abnormal branching pattern in a patient with mild supravalvar aortic stenosis and Williams-Beuren syndrome. Congenit Heart Dis 2014;9:E85-9.

38. Collins RT 2nd, Kaplan P, Somes GW, et al. Long-term outcomes of patients with cardiovascular abnormalities and Williams syndrome. Am J Cardiol 2010;105:874-8.

39. Del Pasqua A, Rinelli G, Toscano A, et al. New findings concerning cardiovascular manifestations emerging from long-term follow-up of 150 patients with the Williams-Beuren-Beuren syndrome. Cardiol Young 2009;19:563-7.

40. Han S, Jeon TY, Hwang SM, et al. Imaging findings of Alagille syndrome in young infants: differentiation from biliary atresia. Br J Radiol 2017;90:20170406.

41. Kohaut J, Pommier R, Guerin F, et al. Abdominal arterial anomalies in children with Alagille syndrome: surgical aspects and outcomes of liver transplantation. J Pediatr Gastroenterol Nutr 2017;64:888-91.

42. Rodriguez RM, Feinstein JA, Chan FP. CT-defined phenotype of pulmonary artery stenoses in Alagille syndrome. Pediatr Radiol 2016;46:1120-7.

43. Rodriguez-Vita J, Tetzlaff F, Fischer A. Notch controls endothelial cells. Oncoscience 2017;4:45-6.

44. Kamath BM, Spinner NB, Emerick KM, et al. Vascular anomalies in Alagille syndrome: a significant cause of morbidity and mortality. Circulation 2004;109:1354-8.

45. Hia CP, Quak SH, Quek SC. Mid aortic syndrome and Alagille syndrome. Heart 2004;90:1150.

46. Monge MC, Mainwaring RD, Sheikh AY, et al. Surgical reconstruction of peripheral pulmonary artery stenosis in Williams and Alagille syndromes. J Thorac Cardiovasc Surg 2013;145:476-81.

47. Hoshino Y, Machida M, Shimano SI, et al. An adult case of chromosome 22q11.2 deletion syndrome associated with a high-positioned right aortic arch. Intern Med 2017;56:865-72.

48. Cuneo BF. 22q11.2 deletion syndrome: DiGeorge, velocardiofacial, and conotruncal anomaly face syndromes. Curr Opin Pediatr 2001;13:465-72.

49. Momma K, Matsuoka R, Takao A. Aortic arch anomalies associated with chromosome 22q11 deletion (CATCH 22). Pediatr Cardiol 1999;20:97-102.

50. Wilson DI, Cross IE, Goodship JA, et al. DiGeorge syndrome with isolated aortic coarctation and isolated ventricular septal defect in three sibs with a 22q11 deletion of maternal origin. Br Heart J 1991;66:308-12.

51. John AS, Rychik J, Khan M, et al. 22q11.2 deletion syndrome as a risk factor for aortic root dilation in tetralogy of Fallot. Cardiol Young 2014;24:303-10.

52. Chan FP, Hanneman K. Computed tomography and magnetic resonance imaging in neonates with congenital cardiovascular disease. Semin Ultrasound CT MR 2015;36:146-60.